

The upper limit on antideuteron flux with BESS-Polar II

K. Sakai ^{*,a,b,*} **K. Abe** ^{†,c} **H. Fuke** ^d **S. Haino** ^{‡,e} **T. Hams** ^{a,b} **M. Hasegawa** ^e
K. C. Kim ^f **M. H. Lee** ^{§,f} **Y. Makida** ^e **J. W. Mitchell** ^a **J. Nishimura** ^{d,g} **M. Nozaki** ^e
R. Orito ^{¶,h} **J. F. Ormes** ⁱ **M. Sasaki** ^{a,b} **E. S. Seo** ^f **R. E. Streitmatter** ^{||,a} **N. Thakur**
****** ^a **A. Yamamoto** ^e **T. Yoshida** ^d and **K. Yoshimura** ^j

^aNASA Goddard Space Flight Center, Astroparticle Physics Laboratory, Greenbelt, MD 20771, USA

^bCenter for Research and Exploration in Space Science and Technology (CRESST)

^cKobe University, Kobe, Hyogo 657-8501, Japan

^dInstitute of Space and Astronautical Science, Japan Aerospace Exploration Agency (ISAS/JAXA),
Sagamihara, Kanagawa 252-5210, Japan

^eHigh Energy Accelerator Research Organization (KEK), Tsukuba, Ibaraki 305-0801, Japan

^fIPST, University of Maryland, College Park, MD 20742, USA

^gThe University of Tokyo, Bunkyo, Tokyo 113-0033, Japan

^hKobe University, Kobe, Hyogo 657-8501, Japan

ⁱUniversity of Denver, Denver, CO 80208, USA

^jOkayama University, Okayama, Okayama 700-8530, Japan

E-mail: kenichisakai@uchicago.edu

*Present address: Enrico Fermi Institute of The University of Chicago, Chicago, IL 60637, USA.

†Present address: Kamioka Observatory, Institute for Cosmic Ray Research, the University of Tokyo, Higashi-Mozumi, Kamioka, Gifu 506-1205, Japan.

‡Present address: Institute of Physics, Academia Sinica, Nankang, Taipei 11529, Taiwan.

§Present address: Center for Underground Physics, Institute for Basic Science (IBS), Daejeon 34126, Korea.

¶Present address: Tokushima University, Tokushima 770-8506, Japan.

|| Deceased.

**Present address: Prince George's Community College, Largo, MD 20774, USA.

*Speaker

In contrast to high-statistics antiproton (\bar{p}) measurements, no cosmic-ray antideuteron (\bar{d}) has been detected. An advantage of the \bar{d} search over the \bar{p} measurement lies in the extremely low astrophysical background of \bar{d} 's, especially at low energy. Before the flight of the next-generation experiment, GAPS, we searched for \bar{d} 's in the 4.7×10^9 cosmic-ray events observed by BESS-Polar II at the solar minimum in 2007. No \bar{d} candidates were detected in the analysis, which adapted a quality cut nearly identical to the BESS-Polar II \bar{p} flux calculation. Thus, the 95% C.L. upper limit on the \bar{d} flux in the energy range from 0.163 to 1.100 GeV/n at the top of the atmosphere was calculated with a conservative analysis. The resultant upper limit was compared to BESS97-00, which currently has the best sensitivity for searching for cosmic-origin \bar{d} 's of $1.9 \times 10^{-4} \text{ (m}^2 \text{ s sr GeV/n)}^{-1}$ and several theories. We will report details of the analysis and the upper limit on \bar{d} flux with BESS-Polar II.



Figure 1: Flight trajectories of the 2007 BESS-Polar II over Antarctica from Williams Field (first orbit blue, second orbit red) with 2004 BESS-Polar I flight (green).

[Launch]S77-51,E166-40, 06:27(McM) 12/23 2007

[Recovery]S83-51,W073-04, 09:02(UTC) 1/21 2008

1. Introduction

The possible presence of various species of antimatter in the cosmic radiation can provide evidence of sources and processes important for both astrophysics and elementary particle physics. Most of the observed cosmic-ray antiprotons (\bar{p} 's) are well understood as secondary products of collisions between primary cosmic-rays and the interstellar medium. The energy spectrum of such “secondary” \bar{p} 's peaks near 2 GeV, and decreases sharply below and above the peak, due to the kinematics of \bar{p} production and to the local interstellar (LIS) proton spectrum. Cosmologically “primary” sources have been suggested, including the annihilation of dark-matter particles and the evaporation of primordial black holes (PBH) by Hawking radiation [1]. While antideuterons (\bar{d} 's) have never been detected in the cosmic radiation, they can be produced by the same sources as \bar{p} 's and may be of both secondary or primary origin, with the latter providing evidence for sources such as PBHs and annihilating neutralino dark matter. The low-energy range below ~ 1 GeV/nucleon offers a unique window in the search for cosmic-ray primary \bar{d} 's because it has a greatly suppressed background from secondary \bar{d} 's. Thanks to their heavier mass, the probability of secondary production in cosmic-ray interactions is much smaller, especially at low energies, because of the very low production cross-section and strict kinematical requirements. Therefore, one single \bar{d} event would be a direct evidence of novel primary origins. The best limit ever achieved was reported by the BESS experiment obtained during last solar minimum period [2].

2. BESS Program

The BESS instrument [3, 4] was developed as a high-resolution magnetic-rigidity spectrometer for cosmic-ray antiparticles and precise measurements of the absolute fluxes of various cosmic-ray components. The original BESS experiment performed 9 flights over northern Canada during the

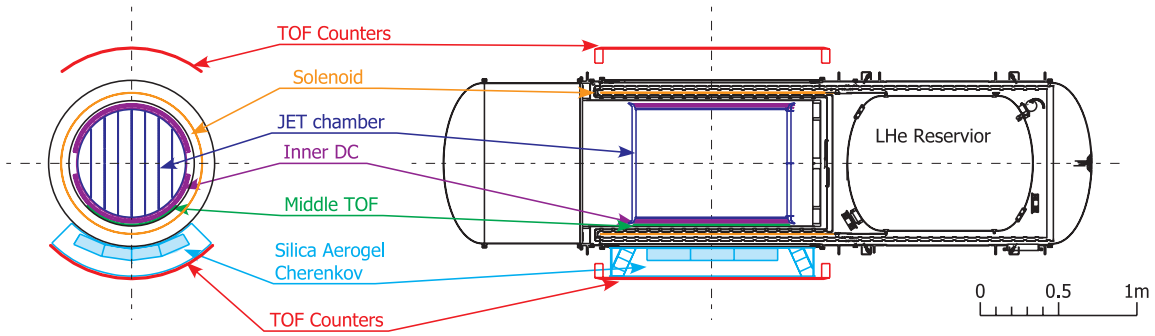


Figure 2: Cross sectional view of BESS-Polar II spectrometer

period of 1993 through 2002 with continuous improvement in the instrument. The BESS-Polar project was proposed as an advanced BESS program using long duration balloon (LDB) flights over Antarctica (around the south pole) to provide high-statistics, low-energy cosmic-ray measurements [5–7]. The first scientific flight of the BESS-Polar instrument was launched near US McMurdo Station in Antarctica, on December 13th, 2004 (UTC). The flight duration was over 8.5 days and more than 9×10^8 cosmic-ray events were recorded [8]. Incorporating considerable improvements in instrument and payload systems compared to BESS-Polar I, the BESS-Polar II instrument was launched on December 23, 2007, from Williams Field near the McMurdo Station and circulated around the South Pole for 24.5 days of observation with the magnet energized. The float altitude was 34 km to 38 km (residual air of 5.8 g/cm^2 on average), and the cutoff rigidity was below 0.5 GV. BESS-Polar II accumulated 4.7×10^9 events with no inflight event selection as 13.6 terabytes of data (Figure 1).

The BESS-Polar II program [9] has published three papers giving precise measurements of \bar{p} [10], a sensitive antihelium search [11] and the absolute spectra measurements for cosmic-ray protons and helium nuclei [12]. The \bar{p} spectrum measured by BESS-Polar II shows good consistency with secondary \bar{p} calculations and no evidence of primary \bar{p} originating from the evaporation of primordial black holes. The antihelium search has set a new limit in the ratio of possible antihelium to measured helium of 6.9×10^{-8} at 95% confidence, the lowest limit to date. Proton and helium spectra observed from PAMELA [13, 14], AMS-02 [15, 16] and BESS-Polar agree within one σ_E at high-energies.

3. BESS-Polar Instrument

In the BESS-Polar instruments shown in Figure 2, a uniform magnetic field of 0.8 T is produced by a thin superconducting solenoid, and the field region is filled with drift-chamber tracking detectors. Tracking is performed by fitting up to 52 hit points with a characteristic resolution of $\sim 140 \mu\text{m}$ in the bending plane, resulting in a magnetic-rigidity ($\equiv Pc/Ze$) resolution of 0.4% at 1 GV and a maximum detectable rigidity (MDR) of 240 GV. Upper and lower scintillator hodoscopes provide time-of-flight (TOF) and dE/dx measurements and the event trigger. For \bar{p} measurements, the acceptance of BESS-Polar is $0.23 \text{ m}^2\text{sr}$ and for proton and helium measurements the acceptance is reduced to be $0.18 \text{ m}^2\text{sr}$. The timing resolution of the TOF system is 120 ps, giving a β^{-1} resolution of 2.5%. The instrument also incorporates a threshold-type Cherenkov counter using a

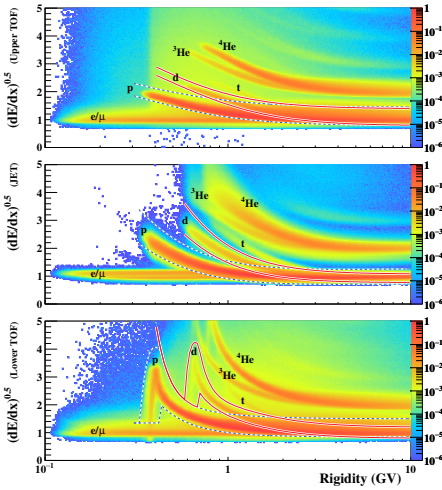


Figure 3: d 's (\bar{d} 's) and p 's (\bar{p} 's) bands in $(dE/dx)^{0.5}$ versus rigidity at the magnet's center (top: Upper TOF, middle: JET, bottom: Lower TOF) from BESS-Polar II.

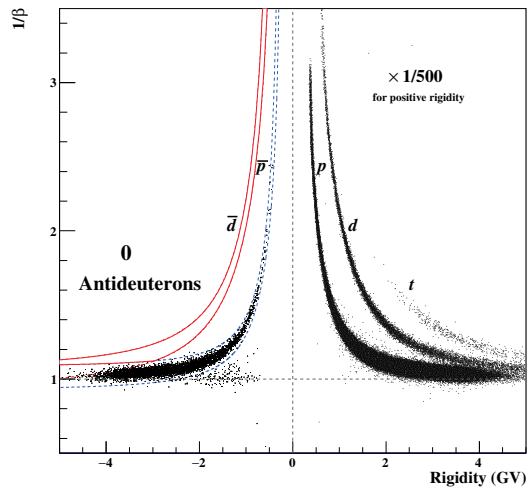


Figure 4: β^{-1} versus rigidity plot at the magnet's center after dE/dx selection for $|Z| = 1$ and Cherenkov veto. There are no \bar{d} 's in the identification region, enclosed by solid lines, defined by excluding the overlapping areas of the \bar{p} band from the \bar{d} band.

silica aerogel radiator with index $n = 1.03$ (ACC) that can reject e^- and μ^- backgrounds by a factor of 12000 and distinguish \bar{p} 's from such backgrounds up to 3.5 GeV. A thin scintillator middle-TOF (MTOF) is installed on the lower inner-surface of the solenoid bore enabling to detect low-energy particles which cannot penetrate the magnet wall. Since readout of both ends of the scintillators was realized for the BESS-Polar II MTOF, it has identical functionalities to the other TOF system including axial position measurements except for inferior timing resolution of 320 ps.

4. The search for \bar{d} 's

In the first stage of data analysis, we selected events with a single track fully contained inside the fiducial volume with acceptable track quality by eliminating the track which scratches the outer most region. A single-track event was defined as an event which has only one isolated track and one or two hit counters in each layer of the TOF hodoscopes. The single-track selection eliminated rare interacting events. To estimate the efficiency of the single-track selection, Monte Carlo simulations with GEANT4 were performed. At this point, the same selection criteria for positive and negative curvature events are applied under the assumption that non-interactive \bar{d} 's behave like deuterons (d 's) except for their deflection thanks to the cylindrical symmetry of the BESS-Polar spectrometer. The selection criteria of \bar{d} are basically identical to what were applied in \bar{p} analysis. To prevent any background contamination into \bar{d} , improved tracking quality was required by eliminating noisy IDC hit events, and selecting events that pass through the center region of JET, and the ACC veto was applied to all energy regions.

From the events surviving quality cuts described above, $(dE/dx)^{0.5}$ band selection was applied to UTOF, JET, and LTOF for \bar{d} (d) particle identification, as shown in Figure 3. Particles pass through in the order stacked in the instrument and stopping can be confirmed in the lower energy

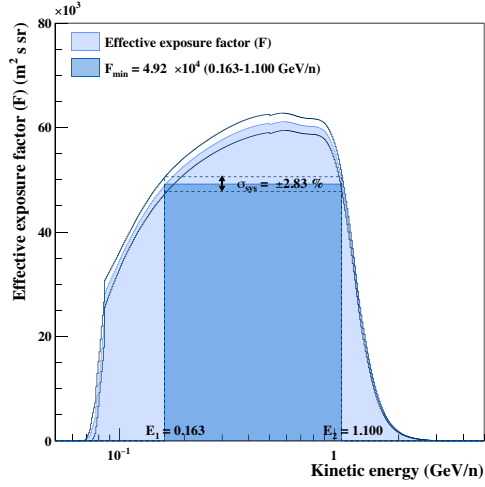
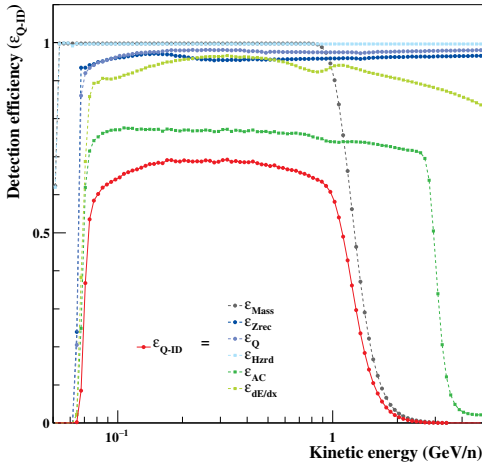


Figure 5: \bar{d} efficiencies of quality and identification cut versus top-of-instrument kinetic energy. They are estimated using d 's in BESS-Polar II area of the rectangle, and the calculated F_{min} is than interaction of the annihilation process.

Figure 6: Effective exposure factor. The energy ranges E_1 and E_2 were selected to maximize the flight, assuming the symmetry of d 's and \bar{d} 's other shown overlaid.

region at the last LTOF. The β^{-1} versus rigidity plot is shown in Figure 4 after applying the $(dE/dx)^{0.5}$ band cut to the positive and negative rigidity regions. The red band indicates the area of \bar{d} with a width of 3.0σ , and the blue band denotes the area of p with a width of 3.5σ . The \bar{d} identification region is within the red band excluding overlap with the blue band to avoid \bar{p} contamination. Consequently, no \bar{d} was found. As the systematic error studies, the \bar{d} search with other conditions was performed, but the results didn't change. Some events near the boundary were investigated but considered to be the tail component of \bar{p} rather than \bar{d} .

5. The upper limit on the \bar{d} flux

Since no \bar{d} was found, an upper limit on the \bar{d} flux was calculated. The contamination from the \bar{p} 's is expected to be 2.72, but the 95% C.L. upper limit is 3.00 in the no signal case, regardless of the background event, because we calculated it using Bayesian statistics assuming a flat prior probability density function [17] rather than the Feldman-Cousin method [18]. Equation 1 is the formula for the upper limit.

$$\Phi_{\bar{d}} = \frac{3.00}{F_{min} \cdot (E_2 - E_1)} \quad (1)$$

$$F_{min} = S\Omega \cdot T_{live} \cdot \varepsilon_{TOI} \cdot \varepsilon_{air} \quad (2)$$

$$\varepsilon_{TOI} = \varepsilon_{Q-ID} \cdot \varepsilon_{other} \cdot \varepsilon_{noint} \quad (3)$$

where F_{min} is minimum effective exposure factor, E_1 and E_2 are both ends of a bin, $S\Omega$ is geometrical acceptance, T_{live} is the live period, ε_{Q-ID} is the detection efficiency of \bar{d} 's, ε_{other} accounts for other

efficiencies described below, $\varepsilon_{\text{noint}}$ is the non-interaction efficiency, ε_{TOI} is the total efficiency at the top of the instrument, ε_{air} is the survival probability in the residual atmosphere.

Figure 5 shows the detection efficiency of the \bar{d} 's calculated with the d 's. The \bar{p} is a more statistic-oriented analysis, with ACC veto only in the higher energy region than 0.8 GeV. In contrast, the \bar{d} has a uniform efficiency because the ACC veto was applied to the entire region to clean up the data.

The analysis using the effective exposure factor is a methodology developed in the BESS97-00 \bar{d} analysis [2]. Basically, the method is to calculate the most conservative upper limit in any one bin from E_1 and E_2 . This provides more robust data when investigating the theory, although it is less sensitive than the previous upper limit calculation because the lowest value is used instead of the average value in the bin, as shown in Figure 6.

6. Conclusion

We will report the 95% C.L. upper limit on the \bar{d} flux in the energy range from 0.163 to 1.100 GeV/n at the top of the atmosphere observed with BESS-Polar II compared to BESS97-00, which currently has the best sensitivity for searching for cosmic-origin \bar{d} 's, and several theories.

Acknowledgements

The BESS-Polar collaboration was supported in Japan by MEXT/JSPS grants KAKENHI (JP13001004; JP18104006; JP19340070; JP22540322), and in the U.S. by NASA (NNX08AC18G; NNX08AD70G; NNX10AC48G; NNX10AG32A; NNX12AH13G; NNX12AI66A). The NASA Columbia Scientific Balloon Facility and the National Science Foundation United States Antarctic Program carried out balloon flight operations. We express our sincere thanks for their continuous, professional support.

References

- [1] S. W. Hawking, *Commun. Math. Phys.* **43**, 199 (1975).
- [2] H. Fuke *et al.*, *Phys. Rev. Lett.* **95**, 081101 (2005).
- [3] Y. Ajima *et al.*, *Nucl. Instrum. Meth.* **A443**, 71 (2000).
- [4] S. Haino *et al.*, *Nucl. Instrum. Meth.* **A518**, 167 (2004).
- [5] A. Yamamoto *et al.*, *Adv. Space Res.* **30**, 1253 (2002).
- [6] J. W. Mitchell *et al.*, *Nucl. Phys. (Proc. Suppl.)* **134**, 31 (2004).
- [7] T. Yoshida *et al.*, *Adv. Space Res.* **33**, 1755 (2004).
- [8] K. Abe *et al.*, *Phys. Lett.* **B670**, 103 (2008).
- [9] K. Abe *et al.*, *Advances in Space Research (In Press)* (2016).

- [10] K. Abe *et al.*, *Phys. Rev. Lett.* **108**, 051102 (2012).
- [11] K. Abe *et al.*, *Phys. Rev. Lett.* **108**, 131301 (2012).
- [12] K. Abe *et al.*, *Astrophys. J.* **822**, 65 (16pp) (2016).
- [13] O. Adriani *et al.*, *Science* **332**, 69 (2011).
- [14] O. Adriani *et al.*, *Phys. Rep.* **544**, 323 (2014).
- [15] M. Aguilar *et al.*, *Phys. Rev. Lett.* **114**, 171103 (2015).
- [16] M. Aguilar *et al.*, *Phys. Rev. Lett.* **115**, 211101 (9pp) (2015).
- [17] I. Narsky, *Nucl. Instrum. Methods Phys. Res. A* **450**, 444 (2000).
- [18] G. J. Feldman, *Phys. Rev. D* **57**, 3873 – 3889 (1998).